Articles

Contribution from the Chemistry Department, University of Auckland, Auckland, New Zealand, Department of Chemistry, University of Southern California, Los Angeles, California 90089-1062, and Battelle-Kettering Laboratory, Yellow Springs, Ohio 45387

Magnetic and Theoretical Studies of the Electronic Structure and Spin State of the Bis(tetrathiomolybdato)iron Trianion, $[Fe(MoS_4)_2]^{3-}$

Graham A. Bowmaker,[†] Peter D. W. Boyd,*[†] Richard J. Sorrenson,[†] Christopher A. Reed,*[‡] and John W. McDonald[§]

Received August 30, 1985

The magnetic susceptibility (1.7–300 K) and low-temperature (1.7–30 K) magnetization (1–4 T) of the bis(tetrathiometalato)iron trianion in polycrystalline $[Et_4N]_3[Fe(MoS_4)_2]$ have been measured. The temperature and field dependence of the magnetization have been analyzed in terms of an $S = {}^3/_2$ orbital singlet ground state with a substantial zero-field splitting, $g = 1.985$ and $D = +4.4$ cm^{-1}. Spin-restricted scattered wave–SCF–Xα calculations of the electronic structure of the $[Fe(MoS_4)_2]^{3-}$ anion (D_{2d} symmetry) suggest that this spin state arises from occupancy of the iron d orbitals by seven electrons leading to a ground-state electron configuration $(z^2)^2(xy)^2(x^2-y^2)^1(xz,yz)^2$ with the three unpaired electrons occupying the b_1 and e orbitals of the iron atom. This leads to the formulation of $[Fe(MoS_4)_2]^{3-}$ as an iron(I) complex coordinated by two $Mo^{VI}S_4^{2-}$ anions. Even though a d^7 configuration is favored, the resulting charge distribution is close to that of analogous d^6 iron(II) $[Fe(MoS_4)(SH)_2]^{2-}$ complexes. The extra charge in the trianion is principally delocalized over the tetrathiomolybdate anions. Spin-polarized calculations lead to similar conclusions concerning the charge distribution with a change in the nature of the LUMO from an iron $(xz,yz)^4$e to a $[(x^2-y^2)^\beta]b_1$ orbital. Calculations of the Mössbauer quadrupole splitting agree well with the experimentally reported value. Contributions to the electric field gradient from both iron p and d electrons are found to be of similar magnitude. Similar calculations on the analogous tungsten complex suggest an explanation for why the isomer shifts of $[Fe(WS_4)_2]^{2-/3-}$ are almost identical, but their quadrupole splittings are markedly different.

Introduction

Recent studies of the enzyme nitrogenase have shown the presence of an iron–molybdenum–sulfur cofactor consisting of a cluster of one molybdenum, six to eight iron, and four to eight sulfur atoms having an overall $S = {}^3/_2$ electronic ground state.[1] This has prompted many attempts to prepare synthetic models of this intriguing molecule.[2] Most of the models so far reported are derived from the tetrathiomolybdate anion, MoS_4^{2-}, a versatile ligand, which when combined with iron gives a variety of multimetallic clusters.[3] The bis(tetrathiomolybdato)iron trianion, $[Fe(MoS_4)_2]^{3-}$, was reported simultaneously by Coucouvanis[4] and by McDonald[5] in 1980. The complex consists of an iron atom tetrahedrally coordinated by two bidentate MoS_4^{2-} groups. The magnetic moment (μ_{eff}) corresponds to three unpaired electrons ($S = {}^3/_2$) and the electron spin resonance (ESR) spectra of frozen solutions correspond to those expected from a spin quartet with a large zero-field splitting relative to the X-band microwave quantum.[6]

The formal oxidation state of the iron atom in $[Fe(MoS_4)_2]^{3-}$ has been the subject of some discussion. It has been suggested on the basis of the iron–sulfur and molybdenum–sulfur bond lengths and Mössbauer isomer shifts that the reduction is centered on the MoS_4^{2-} ligands rather than the central iron atoms.[4,7] This has been attributed to the presence of low-lying empty d orbitals on the molybdenum atom which may be capable of Fe → Mo(VI) charge delocalization.[8] This is similar to results recently found in the case of the one-electron reduction product of $[Ni(MoS_4)_2]^{2-}$ in which the single unpaired electron in $[Ni(MoS_4)_2]^{3-}$ appears to occupy a molecular orbital delocalized over the two molybdenum centers.[9] Three formulations of the $[Fe(MoS_4)_2]^{3-}$ ion that lead to an $S = {}^3/_2$ ground state are possible: a low-spin iron(III) ($S = {}^1/_2$) atom ferromagnetically coupled to two molybdenum(V) ($S = {}^1/_2$) centers; a high-spin iron(III) ($S = {}^5/_2$) atom antiferromagnetically coupled to two molybdenum(V) ($S = {}^1/_2$) centers; and an iron(I) ($S = {}^3/_2$) atom bound by two diamagnetic MoS_4^{2-} ligands. The first of these is extremely unlikely since tetrahedral iron(III) complexes are not expected to be low spin.[10] The second formulation is favored from Mössbauer isomer shift arguments[4,7] and ESR spectroscopy.[6]

In this work we describe studies of the magnetic susceptibility (1.7–300 K) and low-temperature magnetization (1.7–30 K) that unequivocally demonstrate the $S = {}^3/_2$ ground state and the sign of the zero-field splitting for $[Et_4N]_3[Fe(MoS_4)_2]$. Scattered wave–Xα calculations of the electronic structure of the $[Fe(MoS_4)_2]^{3-}$ ion, the related $[Fe(WS_4)_2]^{2-/3-}$ ions, and the $[Fe^{II}(MoS_4)(SH)_2]^{2-}$ ion are then presented which suggest that the complex $[Fe(MoS_4)_2]^{3-}$ should be formulated as an Fe(I) d^7 ($S = {}^3/_2$) complex even though the resultant charge distribution is very similar to analogous iron(II) thiomolybdate complexes.

Experimental Section

$[Et_4N]_3[Fe(MoS_4)_2]$ was prepared by literature methods,[5,6] and all subsequent manipulations were carried out in a helium-filled glovebox (O_2, $H_2O < 1$ ppm). Approximately 25-mg samples of ground microcrystalline were used for magnetic susceptibility studies on an SHE Model 905 SQUID susceptometer. Samples were weighed to within 0.1

[†] University of Auckland.
[‡] University of Southern California.
[§] Battelle-Kettering Laboratory.

(1) Burgess, B. K.; Newton, W. E. *Nitrogen Fixation: The Chemical-Biochemical-Genetic Interface*; Müller, A., Newton, W. E., Eds.; Plenum: New York, 1983; p 83.
(2) (a) Holm, R. H. *Chem. Soc. Rev.* **1981**, *10*, 455. (b) Coucouvanis, D. *Acc. Chem. Res.* **1981**, *14*, 201. (c) Averill, B. H. *Struct. Bonding (Berlin)* **1983**, *53*, 59.
(3) Müller, A.; Diemann, E.; Jostes, R.; Bogge, H. *Angew. Chem., Int. Ed. Engl.* **1981**, *20*, 934.
(4) Coucouvanis, D.; Simhon, E. D.; Baenziger, N. C. *J. Am. Chem. Soc.* **1980**, *102*, 6644.
(5) McDonald, J. W.; Friesen, G. D.; Newton, W. E. *Inorg. Chim. Acta* **1980**, *46*, L79.
(6) Friesen, G. D.; McDonald, J. W.; Newton, W. E.; Euler, W. B.; Hoffman, B. M. *Inorg. Chem.* **1983**, *22*, 2202.
(7) Simopoulos, A.; Papaefthymiou, V.; Kostikas, A.; Petrouleas, V.; Coucouvanis, D.; Simhon, E. D.; Stremple, P. *Chem. Phys. Lett.* **1981**, *81*, 261.
(8) Müller, A.; Sarkar, S. *Angew. Chem., Int. Ed. Engl.* **1977**, *16*, 705.
(9) Bowmaker, G. A.; Boyd, P. D. W.; Campbell, G. K.; Zvagulis, M. *J. Chem. Soc., Dalton Trans.* **1986**, 1065.
(10) Lane, R. W.; Ibers, J. A.; Frankel, R. B.; Papaefthymiou, G. C.; Holm, R. H. *J. Am. Chem. Soc.* **1977**, *99*, 84.

0020-1669/87/1326-0003$01.50/0

Table I. Parameters Used in Scattered Wave–Xα Calculations

	coordinates, au			radius, au
		$[Fe(MoS_4)_2]^{3-}$		
Out	0.0	0.0	0.0	10.782
Fe	0.0	0.0	0.0	2.380
Mo	0.0	0.0	+5.195	2.466
S_B	−2.391	−2.391	2.599	2.496
S_T	−2.394	2.394	7.509	2.544
		$[Fe(MoS_4)(SH)_2]^{2-}$		
Out	0.0	0.0	−0.344	8.640
Fe	0.0	0.0	−2.738	2.424
Mo	0.0	0.0	2.468	2.453
S_B	0.0	−3.356	−0.135	2.489
S_T	3.360	0.0	4.759	2.528
S	3.475	0.0	−5.385	2.517
H	5.638	0.0	−4.070	0.336
		$[Fe(WS_4)_2]^{2-/3-}$		
Out	0.0	0.0	0.0	10.771
Fe	0.0	0.0	0.0	2.398
W	0.0	0.0	5.244	2.538
S_B	2.397	2.397	2.689	2.474
S_T	−2.368	2.368	7.567	2.497

mg and packed tightly into a precalibrated aluminum bucket. The tightly fitting lid was made airtight with a thin smear of epoxy glue whose diamagnetic susceptibility was determined to be negligible. Duplicate sets of data were reproducible to within 3%. A diamagnetic correction of -491×10^{-6} cgs units was used. The g value was calculated from the slope of the Curie plot by using a rearranged form of the standard relationship

$$X_M = \frac{Ng^2\beta^2S(S+1)}{3KT}$$

So-called reduced moments M' were calculated from the relationship $M' = \bar{M}/N$ where $\bar{M}$ is the bulk molar magnetization of the sample.

Calculated powder average magnetizations for the quartet state including zero-field splitting were derived from the basic thermodynamic formula[11,12]

$$\bar{M} = \frac{-N}{4\pi}\int_{\theta=0}^{\pi}\int_{\phi=0}^{2\pi}\{\sum(dE_p/dH)\exp(-E_p/kT)/\sum\exp(-E_p/kT)\}\sin\theta\, d\theta\, d\phi$$

The energies, E_p, of the $S = {}^3/_2$ state were obtained by diagonalization of the quartet state matrix including Zeeman and zero-field splitting term, $D[S_z^2 - {}^1/_3S(S+1)]$, while derivatives were calculated using the Hellmann Feynman Theorem.[13,14] The integral was evaluated numerically.

Details of Calculations

The electronic structures of $[Fe(MoS_4)_2]^{3-}$, $[Fe(WS_4)_2]^{2-/3-}$, and $[Fe(MoS_4)(SH)_2]^{2-}$ were calculated by using the SCF–scattered wave–Xα method[15,16] using the program XASW of Case and Cook.[17,18] The geometric structure of $[Fe(MoS_4)_2]^{3-}$ was taken from that reported by Coucouvanis[4] and idealized to D_{2d} symmetry (Mo–Fe–Mo = 180°) for the calculation (Table I; Figure 1a. The structure of the $[Fe(WS_4)_2]^{2-/3-}$ ions was taken from the reported crystal structure of the trianion.[23] The geometric structure for the $[Fe(MoS_4)(SH)_2]^{2-}$ ion was taken from the reported structure of $[Fe(MoS_4)(SPh)_2]^{2-}$[19] and idealized to C_{2v} symmetry (Table I; Figure 1b). The starting molecular potentials were constructed from a superposition of atomic charge densities using overlapping atomic spheres.[20] The atomic radii were chosen by using the method of Norman[21] as the atomic radii reduced by a factor of 0.88 (Table I). α values were those given by Schwarz.[22] Partial wave expansions were included up to $l = 4$ for the outer sphere, $l = 2$ for the iron atom, and $l = 1$ for the sulfur atoms.

A Watson sphere of radius equal to that of the outer sphere with charge equal in magnitude and opposite in sign to the complex was used.[24] The SCF–scattered wave calculation was continued

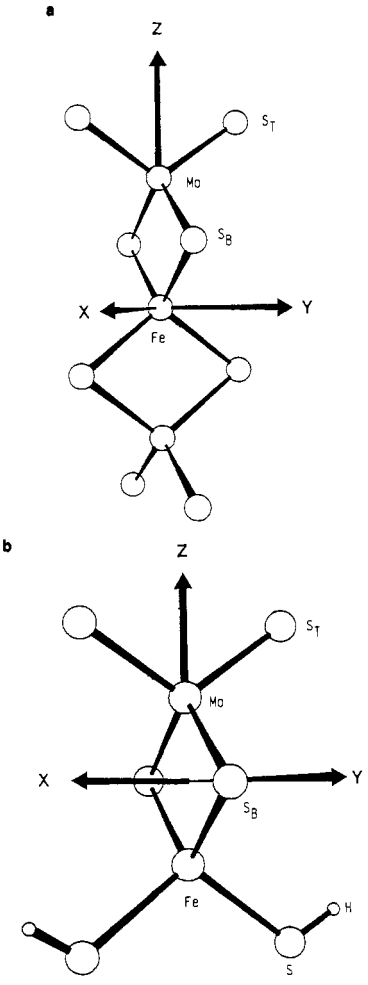

Figure 1. Coordinate system for (a) $[Fe(MoS_4)_2]^{3-}$ and (b) $[Fe(MoS_4)(SH)_2]^{2-}$.

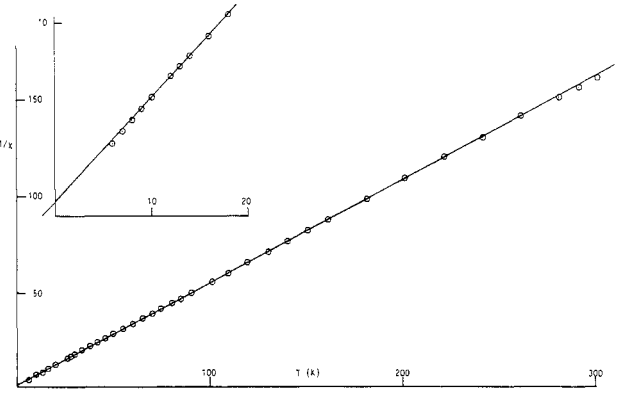

Figure 2. Plot of $1/\chi_M$ vs. T for $[Fe(MoS_4)_2]^{3-}$.

(11) Vermaas, A.; Groeneveld, W. L. *Chem. Phys. Lett.* **1974**, *27*, 583.
(12) Boyd, P. D. W.; Martin, R. L. *J. Chem. Soc., Dalton Trans.* **1979**, 92.
(13) Atkins, P. W. *Molecular Quantum Mechanics*, 1970. Oxford University Press, p 216.
(14) Gerloch, M.; McMeeking, R. F. *J. Chem. Soc., Dalton Trans.* **1975**, 2443.
(15) Johnson, K. H. *Adv. Quantum Chem.* **1973**, *7*, 143.
(16) Case, D. A. *Annu. Rev. Phys. Chem.* **1982**, *33*, 151.
(17) Cook, M.; Case, D. A. Program XASW Version 2.
(18) Case, D. A.; Cook, M.; Karplus, M. *J. Chem. Phys.* **1980**, *73*, 3294.
(19) Coucouvanis, D.; Stremple, P.; Simhon, E. D.; Swenson, D.; Baenziger, N. C.; Draganjac, M.; Chan, L. T.; Simopoulos, A.; Papaefthymiou, V.; Kostikas, A.; Petrouleas, V. *Inorg. Chem.* **1983**, *22*, 293.
(20) Herman, F.; Williams, A. R.; Johnson, K. H. *J. Chem. Phys.* **1974**, *61*, 3508.
(21) Norman, J. G., Jr. *J. Chem. Phys.* **1974**, *61*, 4630.
(22) Schwarz, K. *Phys. Rev. B: Solid State* **1972**, *5*, 2446.
(23) McDonald, J. W.; Friesen, G. D.; Müller, A.; Hellmann, W.; Schimanski, V.; Trautwein, A.; Bender, U. *Inorg. Chim. Acta* **1983**, *76*, L297.
(24) Watson, R. E. *Phys. Rev.* **1958**, *111*, 1108.

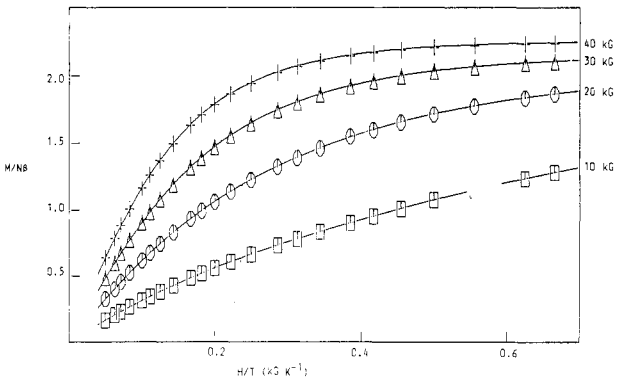

Figure 3. Calculated (g = 1.985 and D = 4.4 cm^{-1}) and observed reduced magnetizations as a function of field and temperature.

until the relative change in potential at all points in the complex was less than 10^{-4}. Charge distributions and electric field gradients were calculated by using the charge-partitioning method of Case, Cook, and Karplus.[25,26] Mössbauer quadrupole splittings were calculated from the formula[27,28]

$$\Delta E_Q = \tfrac{1}{2}e^2Q(1 - \gamma_0)q(1 + \eta^2/3)^{1/2}$$

where $\eta = (V_{xx} - V_{yy})/V_{zz}$, $eq = V_{zz}$, V_{ii} = field gradient in the ith direction, Q is the quadrupole moment of the iron nucleus, and $(1 - \gamma_0)$ is the Sternheimer antishielding factor.[29] The product of Q and $(1 - \gamma_0)$ has been taken as 0.143.[30,31]

Results

Magnetic Susceptibility and Magnetization. The magnetic susceptibility of $[Et_4N]_3[Fe(MoS_4)_2]$ in the temperature range 200–6 K obeys the Curie–Weiss law with C = 1.853 ± 0.002 and Θ = −1.41 ± 0.09 K. Data are displayed graphically in Figure 2 and are listed in Table IIa of the supplementary material. This behavior corresponds closely to that expected for an isolated spin quartet ($S = {}^3/_2$) orbitally nondegenerate ground state. The g value calculated from the slope of the linear portion of the Curie–Weiss plot, g = 1.988, agrees well with that reported for this type of complex in ESR studies.[6] At higher temperatures the plot of $1/\chi$ against T is slightly nonlinear probably due to temperature-independent paramagnetism contributions to the susceptibility. The magnetic moments calculated from these susceptibilities are nearly constant over the range 300 (3.86 μ_B) to 70 K (3.80 μ_B). They are listed in Table IIa of the supplementary material. At lower temperatures the magnetic moment decreases with decreasing temperature as would be expected for such an $S = {}^3/_2$ state with significant zero-field splitting.

Measurement of the temperature and field dependence of the magnetization, $\bar{M}$, of $[Et_4N]_3[Fe(MoS_4)_2]$ from 1.7 to 30 K and 1 to 4 T (Table IIb of the supplementary material) allows evaluation of the magnitude and the sign of the zero-field splitting. A model involving a single $S = {}^3/_2$ multiplet with axial zero-field splitting was used to calculate the powder-averaged magnetization $\bar{M}$ for comparison with experiment (eq 1). Figure 3 shows that a model (solid lines) with g = 1.985 ± 0.002 and D = +4 ± 0.1 cm^{-1} accounts well for the experimental data. The fit is moderately sensitive to simultaneous variation of g and D enabling us to narrow the range of acceptable fits to g values in the range 1.90–1.99 and D in the range 4.0–4.4 cm^{-1}. The fit to the magnetization data in Figure 3 unequivocally determines an $S = {}^3/_2$ ground state for the $[Fe(MoS_4)_2]^{3-}$ ion. The positive sign of D is in accord with indications from ESR data.[6]

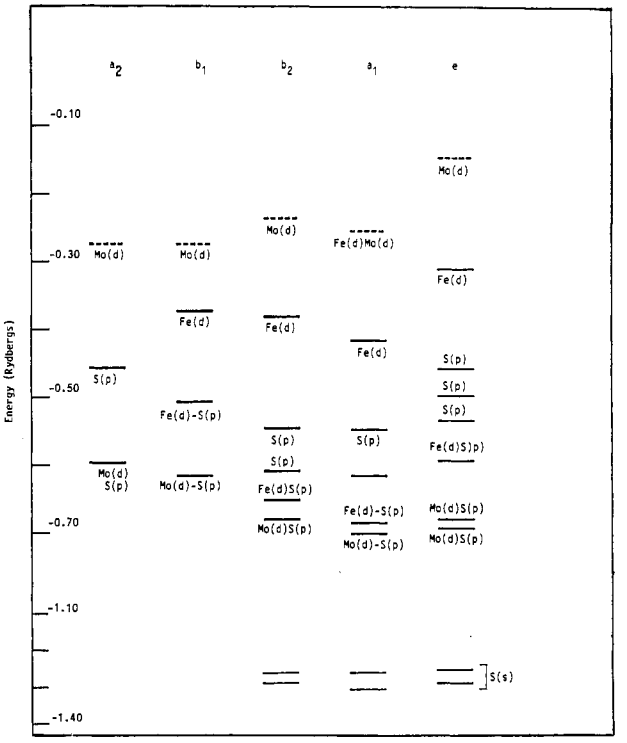

Figure 4. Xα valence orbital energies for $[Fe(MoS_4)_2]^{3-}$ (restricted SW–Xα calculation). The main character of the orbitals is indicated. Dashed lines represent vacant orbitals.

Orbital Energies and Wave Functions. Spin-Restricted Calculation. The spin-restricted Xα valence orbital energies calculated for the $[Fe(MoS_4)_2]^{3-}$ trianion are shown in Figure 4 and are listed in Table IIIa of the supplementary material. The highest occupied levels of $[Fe(MoS_4)_2]^{3-}$ are principally based on the d orbitals of the iron atom while the low-lying unoccupied levels are largely based on the d orbitals of molybdenum atoms. The three unpaired electrons occupy the 9e and $3b_1$ levels that correspond to (xy,yz) and $(x^2 - y^2)$ orbitals of the iron atom, respectively. The $3b_1$ and $7b_2$ levels are close in energy and the ground-state configuration $(3b_1)^1(9e)^2$ was confirmed by a transition-state calculation between the $3b_1$ and $7b_2$ levels.[32]

Ligand field theory (LFT) predicts that the relative ordering of the d orbitals in a tetrahedral field is e < t_2. These split in D_{2d} symmetry (e → a_1 + b_1 and t_2 → e + b_2). The relative ordering of the iron orbitals, from the restricted calculation in $[Fe(MoS_4)_2]^{3-}$ is 9e > $3b_1$ > $7b_2$ > $7a_1$ as shown in Figure 5. This order varies slightly from that found in recent Fenske–Hall LCAOMO[33] calculation of $[Fe(MoS_4)_2]^{3-}$, where the $3b_1$ and $7b_2$ orbitals were reversed in order but close in energy and led to the unpaired electron configuration $(7b_2)^1(9e)^2$.[34]

The spin-restricted valence orbital energies calculated for $[Fe(WS_4)_2]^{3-}$ are very similar to those found for $[Fe(MoS_4)_2]^{3-}$ and are listed in Table IIIb of the supplementary material. The analogous $[Fe(WS_4)_2]^{2-}$ anion has a similar ordering of levels to the trianion but with four unpaired electrons occupying the iron "d orbitals" to give a ground-state configuration $(z^2)^2(xy)^1(x^2 - y^2)^1(xz,yz)^2$ (Table IIIc).

The ordering of levels in $[Fe(MoS_4)(SH)_2]^{2-}$ (Figure 6) is similar to that of the $[Fe(MoS_4)_2]^{2-}$ ion with the vacant molybdenum d orbitals lying above the singly occupied d levels of the iron atom (Table IIId). In this case there are four unpaired electrons occupying the iron d orbitals leading to a ground configuration from the restricted calculation $(10a_1)^2(4a_2)^1(11a_1)^1(6b_2)^1(8b_1)^1$ corresponding to $(z^2)^2(xy)^1(x^2 - y^2)^1(yz)^1(xz)^1$.

(25) Case, D. A.; Karplus, M. *Chem. Phys. Lett.* **1976**, *39*, 33.
(26) Cook, M.; Karplus, M. *J. Chem. Phys.* **1980**, *72*, 7.
(27) Trautwein, A. *Struct. Bonding (Berlin)* **1974**, *20*, 101.
(28) e^2qQ/h (MHz) = 234.9eq (au) × Q (b).
(29) Lucken, E. A. C. *Nuclear Quadrupole Coupling Constants*; Academic Press: London, 1969; p 79.
(30) Case, D. A.; Huynh, B. H.; Karplus, M. *J. Am. Chem. Soc.* **1979**, *101*, 4433.
(31) Sontum, S. T.; Case, D. A. *J. Chem. Phys.* **1983**, *79*, 2881.
(32) Slater, J. C. *Adv. Quantum Chem.* **1972**, *6*, 1.
(33) Fenske, R. F.; Hall, M. B. *Inorg. Chem.* **1972**, *11*, 768.
(34) Szterenberg, L.; Jezowska-Trzebiatowska, B. *Inorg. Chim. Acta* **1984**, *86*, L29.

Table IV

a. Gross Iron Atomic Orbital Populations for $[Fe(MoS_4)_2]^{3-}$, $[Fe(WS_4)_2]^{3-}$, $[Fe(WS_4)_2]^{2-}$, and $[Fe(MoS_4)(SH)_2]^{2-}$ [a]

iron orbital	$[Fe(MoS_4)_2]^{3-}$	$[Fe(WS_4)_2]^{3-}$	$[Fe(WS_4)_2]^{3-}$	$[Fe(MoS_4)(SH)_2]^{2-}$
s	0.533 (0.539)	0.502 (0.517)	0.506 (0.523)	0.516 (0.553)
p_z	0.277 (0.275)	0.284 (0.277)	0.236 (0.240)	0.224 (0.239)
p_x, p_y	0.226 (0.237)	0.216 (0.225)	0.215 (0.224)	0.237[b] (0.248)
				0.258[c] (0.285)
d_{z^2}	1.622 (1.586)	1.669 (1.651)	1.757 (1.763)	1.696 (1.454)
d_{xz}, d_{yz}	1.338 (1.284)	1.328 (1.255)	1.389 (1.319)	1.386[d] (1.315)
				1.361[e] (1.322)
d_{xy}	1.565 (1.555)	1.670 (1.645)	1.379 (1.226)	1.308 (1.229)
$d_{x^2-y^2}$	1.267 (1.178)	1.232 (1.146)	1.175 (1.183)	1.236 (1.356)

b. Gross Atomic Populations[f] for $[Fe(MoS_4)_2]^{3-}$, $[Fe(WS_4)_2]^{3-}$, $[Fe(WS_4)_2]^{2-}$, and $[Fe(MoS_4)(SH)_2]^{2-}$

		$[Fe(MoS_4)_2]^{3-}$	$[Fe(WS_4)_2]^{3-}$	$[Fe(WS_4)_2]^{2-}$	$[Fe(MoS_4)(SH)_2]^{2-}$
Fe	s	0.533 (0.539)	0.502 (0.512)	0.505 (0.524)	0.517 (0.554)
	p	0.728 (0.748)	0.715 (0.725)	0.665 (0.689)	0.720 (0.774)
	d	7.130 (6.887)	7.225 (6.955)	7.092 (6.808)	6.987 (6.678)
Mo	s	0.473 (0.429)	0.537 (0.486)	0.530 (0.477)	0.470 (0.466)
	p	0.557 (0.547)	0.648 (0.638)	0.627 (0.616)	0.563 (0.559)
	d	4.451 (4.344)	4.353 (4.225)	4.311 (4.166)	4.442 (4.412)
S_B	s	1.841 (1.830)	1.826 (1.807)	1.825 (1.809)	1.813 (1.800)
	p	4.474 (4.536)	4.502 (4.540)	4.429 (4.486)	4.497 (4.557)
S_T	s	1.842 (1.832)	1.803 (1.796)	1.804 (1.792)	1.835 (1.833)
	p	4.755 (4.740)	4.740 (4.747)	4.642 (4.641)	4.774 (4.744)

[a] Values for restricted calculations in parentheses. [b] p_x. [c] p_y. [d] d_{xz}. [e] d_{yz}. [f] Values for unrestricted calculations in parentheses. ($[Fe(MoS_4)(SH)_2]^{2-}$: SH, s 1.738 and p 4.628; H, s 0.867).

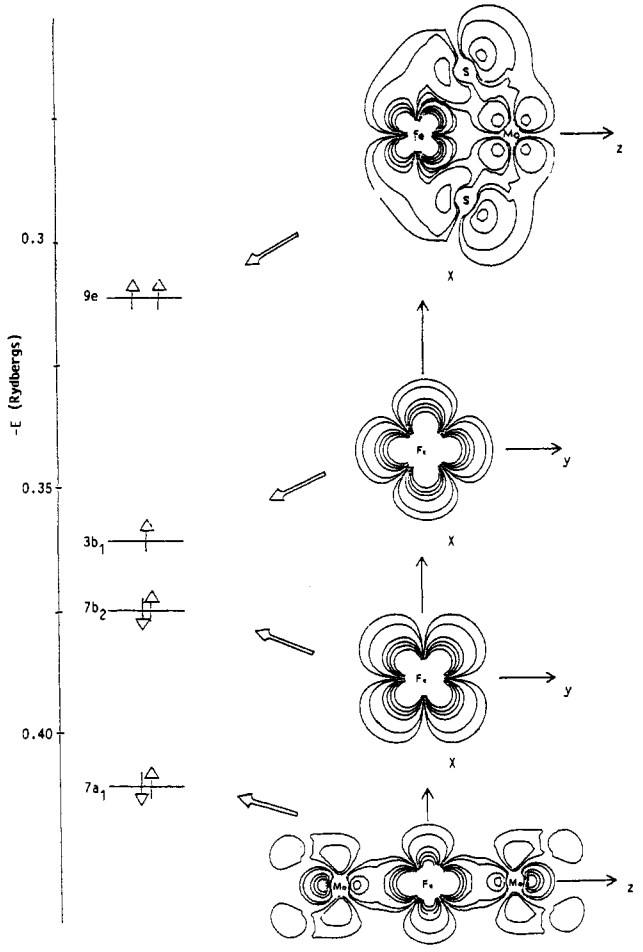

Figure 5. Relative ordering and contour plots of orbitals of mainly iron 3d character in $[Fe(MoSo_4)_2]^{3-}$ for restricted calculation.

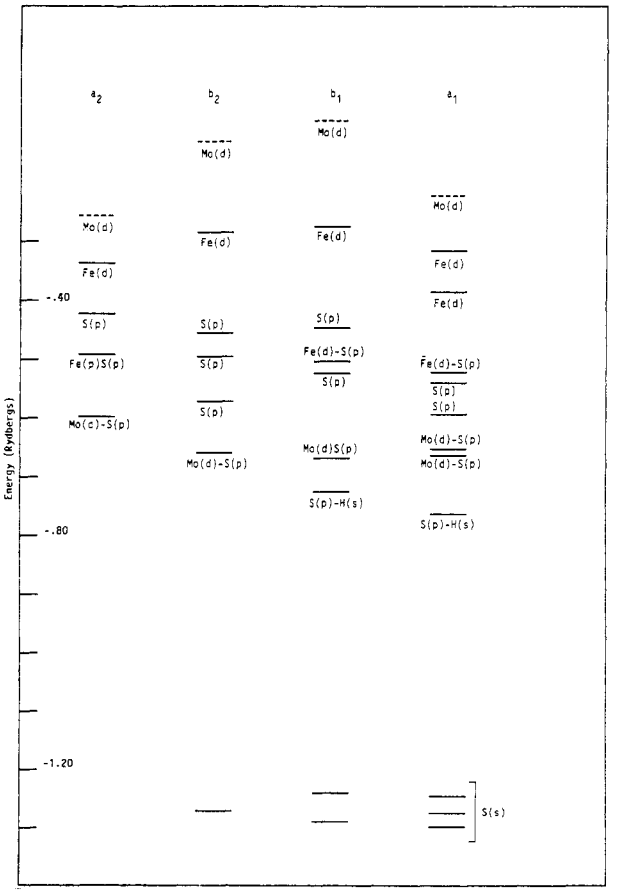

Figure 6. Xα valence orbital energies for $[Fe(MoS_4)(SH)_2]^{2-}$ (restricted calculation). Dashed lines represent vacant orbitals.

Thus from electron configuration considerations $[Fe(MoS_4)_2]^{3-}$ and $[Fe(WS_4)_2]^{3-}$ may be formulated as iron(I) complexes while $[Fe(WS_4)_2]^{2-}$ and $[Fe(MoS_4)(SH)_2]^{2-}$ may be formulated as iron(II) complexes. In the latter regard complexes of the type $[Fe(MoS_4)(SR)_2]^{2-}$ are considered to be tetrahedral iron(II) complexes from magnetic and Mössbauer studies.[19]

The charge distributions in $[Fe(MoS_4)_2]^{3-}$, $[Fe(WS_4)_2]^{2-/3-}$, and $[Fe(MoS_4)(SH)_2]^{2-}$ calculated by the partitioning method of Case, Cook, and Karplus are given in Table IV for the restricted calculations. The gross orbital populations for the iron atom and gross atomic populations for the molecules are given in Table IV together with those of the isolated MoS_4^{2-} ion.[9]

The gross populations of the iron, molybdenum, and thiomolybdate sulfur atoms for all complexes are similar although

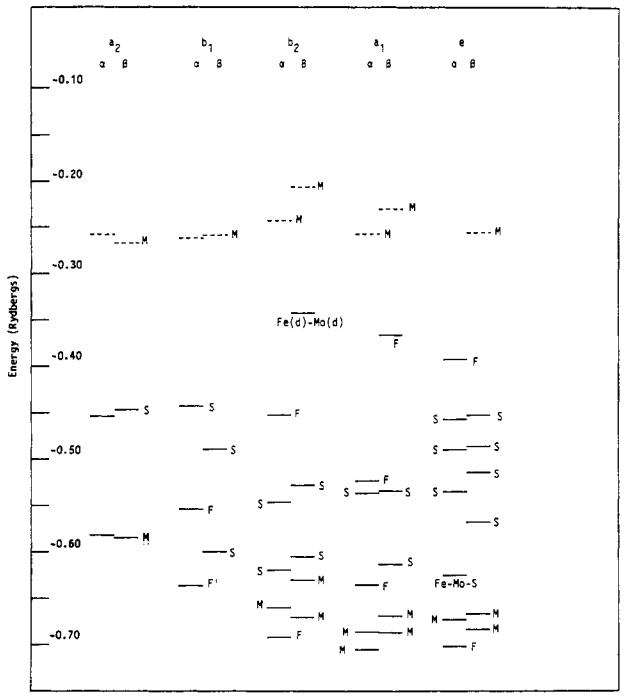

Figure 7. Xα valence orbital energies for $[Fe(MoS_4)_2]^{3-}$ (spin-polarized calculation). Dashed lines represent vacant orbitals. (M = Mo(d)–S(p); S = S(p); F = Fe(d)–S(p); F′ = Fe(d).)

formally they are considered as iron(I) and iron(II) species.

Spin-Polarized Calculation. Spin-polarized Xα calculations combined with transition-state calculations were performed for all four of the above complexes to ensure the correct ground states had been obtained for each of the paramagnetic molecules by using the restricted method. In these calculations the α and β spin orbitals are no longer constrained to have the same radial wave functions.[35] This leads to a stabilization, via greater exchange interactions, of the excess spin functions. In each of the cases studied here these are the α spin orbitals.

The spin-polarized Xα orbital energies for $[Fe(MoS_4)_2]^{3-}$ are given in Figure 7. The relative energies of the sulfur α and β spin orbitals are little affected. However, the Xα orbitals involving iron and the sulfur p orbitals are markedly changed in both energy and composition. The ground-state configuration for the complex is found to be a spin quartet with the same overall configuration for the restricted calculation. There is, however, a differing order of frontier orbitals within this configuration $[...(9e^{\alpha})^2(7a_1^{\beta})^1(7b_2^{\beta})^1]$. The HOMO from the restricted calculation was found to be the $9e^{\beta}$ orbitals while in the spin-polarized method it is the $7b_2^{\beta}$.

The energies of the α and β spin orbitals behave in a similar manner to those reported in other spin-polarized studies of iron sulfur and iron molybdenum sulfur clusters such as the $[Fe_4S_4]^{3-}$ and $[MoFe_3S_4(SH)_6]^{3-}$ ions.[36,37] The α spin orbitals with a large amount of iron d character are in general stabilized more relative to those with a majority of molybdenum d or sulfur p character. Associated with this lowering is a decrease in iron d character of these orbitals and an increase in iron d character of some of the lower sulfur-containing orbitals. This has been explained by Cook and Karplus in terms of the relative energies of the iron d and sulfur p orbitals under spin polarization.[37] Increased stabilization of α spin iron d atomic orbitals relative to sulfur p leads to a greater mixing between them and hence to a greater delocalization of α spin charge in the complex. In contrast the β spin iron d orbitals are at higher energies and combine with sulfur p orbitals in a manner similar to that found in the restricted calculation. Thus in Figure 7 the relative ordering and composition of the β spin orbitals are similar to that found in the restricted calculation while the iron d character of the lower lying α spin orbitals changes markedly.

Similar changes in α and β spin orbital energies and composition are found for $[Fe(WS_4)_2]^{2-/3-}$ and $[Fe(MoS_4)(SH)_2]^{2-}$. In the first two cases there are no major changes to the overall charge distribution and gross iron orbital populations (Table IV) relative to the restricted calculation. The same is found for $[Fe(MoS_4)(SH)_2]^{2-}$ except for changes in the population of iron (z^2) and ($x^2 - y^2$) orbitals discussed in the next section. In each case the same overall electron configurations and spin states as the restricted calculations are found.

Table V. Calculated and Observed Quadrupole Splittings for $[Fe(MoS_4)_2]^{3-}$, $[Fe(WS_4)_2]^{2-/3-}$, and $[Fe(MoS_4)(SH)_2]^{2-}$ Ions

	restricted	unrestricted	expt[g]
$[Fe(MoS_4)_2]^{3-}$			
V_{zz} (au)	−0.799	−0.744	
ΔE_Q (mm s^{-1})	−1.16	−1.08	1.04[a]
$[Fe(WS_4)_2]^{3-}$			
V_{zz} (au)	−0.748	−0.756	
ΔE_Q (mm s^{-1})	−1.08	−1.10	1.03[b]
$[Fe(WS_4)_2]^{2-}$			
V_{zz} (au)	−1.964	−2.066	
ΔE_Q (mm s^{-1})	−2.85	−3.00	2.65[b]
$[Fe(MoS_4)(SH_2)]^{2-}$			
V_{zz} (au)[c]	−1.609 (0.20)[e]	+0.988 (0.318)[f]	
ΔE_Q (mm s^{-1})[c]	−2.34	+1.45	+1.96 (0.1)[d]

[a] For $(Et_4N)_3[Fe(MoS_4)_2]$ at 77 K.[3b] [b] For $(PNP)_2[Fe(WS_4)_2]$ and $(Et_4W)_3[Fe(WS_4)_2]$.[23] [c] Asymmetry parameter in parentheses. [d] For $(Ph_4P)_2[Fe(MoS_4)(SPh)_2]$ a 4.2 K.[19] [e] Principal component along z axis. [f] Principal component along x axis. [g] Signs only included if known.

Nuclear Quadrupole Splitting and Electric Field Gradients. The observed isomer shifts for $[Fe(MoS_4)_2]^{3-}$, $[Fe(WS_4)_2]^{3-/2-}$, and $[Fe(MoS_4)(SR)_2]^{2-}$ (R = Ph) are remarkably similar[2,4,7,19] and indicate that the charge at the iron nucleus is similar in these molecules. This is confirmed in the calculations reported here. The calculated charge on the iron atom and the charge density at the iron nucleus are very close in value. However, the observed quadrupole splittings (Table V) indicate very different iron atom orbital populations for the formally iron(I) $[Fe(MoS_4)_2]^{3-}$ and $[Fe(WS_4)^2]^{3-}$ complexes compared with the formally iron(II) $[Fe(WS_4)^2]^{2-}$ and $[Fe(MoS_4)(SH)_2]^{2-}$ complexes. For investigation of this observation, the electric field gradients and nuclear quadrupole splittings at the iron nucleus were calculated by using the method of Case, Cook, and Karplus[25,26,34] from the Xα wave functions.

The calculated and observed values of the iron Mössbauer quadrupole splitting for each of the above complexes are given in Table V. The agreement for the bis(tetrathiometalate) complexes with the experimentally reported values is quite reasonable for both the restricted and spin-polarized calculations. The calculated values for the $[Fe(MoS_4)(SH)_2]^{2-}$ complex varied in sign and direction of the principal component of electric field gradient from the restricted to spin-polarized calculation. This variation will be discussed later.

The sums of the one-center valence orbital field gradient integrals for the iron atom in $[Fe(MoS_4)_2]^{3-}$ and $[Fe(WS_4)^2]^{2-/3-}$ are equal to the total (electronic, nuclear) field gradients to within 1–2%. This indicates that the occupied valence orbitals centered on the iron atom are the major contributors to the field gradient at the iron nucleus. This has been found in several recent studies of the nuclear quadrupole coupling in halogen-containing molecules[38] and enables a discussion of the field gradient and quadrupole splitting in terms of one-center contributions at the quadrupolar nucleus. These are summarized in Table VI where the average field gradients per electron eq_i are given for each

(35) Wood, J. H.; Pratt, G. W. *Phys. Rev.* **1957**, *107*, 995.
(36) Aizman, A.; Case, D. A. *J. Am. Chem. Soc.* **1982**, *104*, 3269.
(37) Cook, M.; Karplus, M. *J. Am. Chem. Soc.* **1985**, *107*, 257; *J. Chem. Phys.* **1985**, *83*, 6344.
(38) Bowmaker, G. A.; Boyd, P. D. W.; Sorrenson, R. J. *J. Chem. Soc., Faraday Trans. 2* **1984**, 1125.

Table VI. Contributions (One Center) to Electric Field Gradient *eq* for Iron in $[Fe(MoS_4)_2]^{3-}$, $[Fe(WS_4)_2]^{3-}$, $[Fe(WS_4)_2]^{2-}$, and $[Fe(MoS_4)(SH)_2]^{2-}$

	$[Fe(MoS_4)_2]^{3-}$				$[Fe(WS_4)_2]^{3-}$				$[Fe(WS_4)_2]^{2-}$				$[Fe(MoS_4)(SH)_2]^{2-}$			
	eq^a		eq_i		eq^a		eq_i		eq^a		eq_i		eq^a		eq_i	
orbital	res	unres	res	unres	res	unres	res	unres	res	unres	res	unres	res	unres	res	unres
$4p_z$	−2.133	−2.186	−7.700	−7.949	−2.048	−2.096	−7.211	−7.567	−1.835	−1.952	−7.775	−8.133	−1.627	0.895	−7.263	−7.490
$4p_x$, $4p_y$	0.859	0.909	−7.602	−7.671	0.771	0.813	−7.139	−7.227	0.779	0.828	7.247	7.393	0.773	−1.651[b]	6.523	6.657[b]
													0.843	0.902[c]	6.535	6.330[c]
$3d_{z^2}$	−4.179	−4.184	−2.576	−2.638	−4.246	−4.311	−2.544	−2.611	−4.598	−4.721	−2.617	−2.678	−4.477	1.973	−2.640	−2.714
$3d_{xz}$, $3d_{yz}$	−1.674	−1.671	2.503	−2.603	−1.643	−1.628	−2.474	−2.594	−1.766	−1.734	−2.543	−2.629	−1.800	−1.774[d]	−2.597	−2.698[d]
													−1.689	3.422[e]	−2.482	−2.604[e]
$3d_{xy}$	3.899	4.003	2.491	2.574	4.167	4.237	2.495	2.576	2.879	3.126	2.088	2.550	3.342	−1.650	2.555	2.685
$3d_{x^2-y^2}$	3.230	3.137	2.549	2.663	3.111	3.035	2.525	2.648	3.548	3.278	3.020	2.771	3.016	−1.772	2.440	2.614

[a] Principal axes of restricted and unrestricted calculations are *z* and *x*, respectively. [b] p_x. [c] p_y. [d] d_{xz}. [e] d_{yz}.

Table VII. α–β Orbital and Gross Spin Populations for the $[Fe(WS_4)_2]^{2-/3-}$ Ions

	$[Fe(WS_4)_2]^{3-}$				$[Fe(WS_4)_2]^{2-}$			
	Fe	W	S_B	S_T	Fe	W	S_B	S_B
s	0.011	−0.005	0.003	0.0	0.021	−0.002	0.002	−0.001
p	0.113	−0.003	0.110	0.110	0.162	0.008	0.168	0.047
s	2.625	−0.22			2.998	−0.030		
total	2.888	−0.228	0.113	0.029	3.181	−0.024	0.170	0.046

atomic orbital *i* ($eq_i = V_{jj}/n_i$, where *j* = prinicipal symmetry axis of orbital, V_{jj} = total one center field gradient integral for orbital *i* in the direction *j*, and n_i = gross population *i*).

The field gradients at the iron nucleus in $[Fe(MoS_4)_2]^{3-}$ and $[Fe(WS_4)_2]^{2-\beta-}$ are composed of one center contributions from *both the iron p and d orbitals that are of comparable magnitude and sign.* The large contribution to *eq* from the iron p orbitals arises from unequal occupation of the p_x, p_y vs. p_z orbitals (Table IV), and the highly contracted nature of these orbitals. A feature of scattered wave–Xα calculations is the radial flexibility of atomic orbitals on each center.

The Mössbauer quadrupole splitting for $[Fe(MoS_4)(SH)_2]^{2-}$ ion was calculated by assuming only population of the ground state quintet ($S = 2$) state. The temperature dependence of the magnetic susceptibility and quadrupole splitting[19] indicates that the formal oxidation state of the iron is +2 and that the nearest excited state is well removed from the ground quintet state. Transition-state calculations[32] for both restricted and unrestricted potentials indicate this to be so with the difference between the ground and the first excited configuration being greater than 5000 cm^{-1} in each case, indicating thermal population of the ground state only at normal temperatures. While the calculated electric field gradients and quadrupole coupling constants of the bis(tetrathiomolybdate) and bis(tetrathiotungstate) complexes of iron varied only slightly between the restricted and unrestricted models, this was not found to be the case for the $[Fe(MoS_4)(SH)_2]^{2-}$ ion. In the restricted model the principal value of the field gradient, *eq*, is negative and is oriented along the Fe–Mo vector, the *z* axis in our coordinate system, while for the spin-polarized case it is positive and perpendicular to the Fe–Mo vector along the *x* axis. The reported sign of *eq* for the $[Fe(MoS_4)(SH)_2]^{2-}$ ion is positive.[19] A detailed analysis of the gross iron orbital populations and contributions to the field gradient at the iron nucleus for the restricted and spin-polarized calculations indicates that this change in sign and orientation of *eq* arises mainly from variation in the relative contributions of the electrons occupying the (z^2) and $(x^2 - y^2)$ orbitals. Further, this variation is due to differing populations of these two iron orbitals between the two calculations (a decrease of 0.24e for the (z^2) and an increase of 0.12e for the $(x^2 - y^2)$. A feature of interest in the comparison is that contributions to the *xx* and *yy* components of the field gradient (in the molecular axis frame) occur not only from diagonal integrals with respect to the z^2 and $x^2 - y^2$ orbitals but also from off-diagonal terms $\langle\phi_i|F|\phi_j\rangle$ (F = field gradient operator). Terms involving cross-matrix elements of iron s and z^2 orbitals are negligible but those involving z^2 and $x^2 - y^2$ are not. Further, the magnitude of these latter cross terms varies between the restricted and spin-polarized calculations in a similar manner to the diagonal terms. These also contribute significantly to the change in sign and direction of *eq*.

Recent extended Hückel calculations of the electronic structure and electric field gradients at the iron nucleus in $[Fe(MoS_4)(SPh)_2]^{2-}$ appeared during the course of this work.[39] A feature of the calculations was the calculated orientation of *eq* perpendicular to the Fe–Mo vector as found for the spin-polarized SW–Xα calculations reported here. Similar calculations on the iron(II) complex $[Fe(MoS_4)Cl_2]^{2-}$ gave a similar orientation for *eq*. Single-crystal Mössbauer measurements in this complex confirmed the predicted sign and orientation of the principal component of the field gradient.[40] Analogous scattered-wave calculations agree well with the experimentally determined values in this complex.[41]

Discussion

The relative orderings of the iron 3d and molybdenum 4d orbitals given by these calculations are in good agreement with the qualitative scheme proposed by Coucouvanis[2b] for iron thiomolybdate complexes and the calculations of Szterenberg and Jezowska-Trzebiatowsak.[34] The partially occupied iron 3d orbitals are found to lie for the restricted calculations between the occupied sulfur ligand orbitals and the unoccupied molybdenum 4d orbitals. Analogous calculations for the tetrathiotungstate complexes $[Fe(WS_4)_2]^{2-/3-}$ also reveal a similar sequence.

In all the $[Fe(MoS_4)_2]^{3-}$, $[Fe(WS_4)_2]^{2-/3-}$, and $[Fe(MoS_4)(SH)_2]^{2-}$ molecules the whole integer occupations of the iron "d orbitals" approximate to d^7 or d^6 configurations. These configurations correspond to formal oxidation states +1 and +2, respectively. The charges on the iron atoms in all four of the complexes are very similar and are close to neutrality.[37] An examination of the atomic spin populations (from the spin-polarized calculations) indicates that the spin density is highly localized on the iron atoms in d orbitals (Table VII). In the case of $[Fe(MoS_4)_2]^{3-}$ a net d spin density of +2.95 α–β electrons is found compared with +3.0 expected from formal iron oxidation state considerations. A comparison of the spin distributions for $[Fe(WS_4)_2]^{2-/3-}$ (Table VII) shows the α spin density is more delocalized from the iron atom in the dianion than the trianion onto the bridging and terminal sulfur atoms while the net spin

(39) Trautwein, A. X.; Bill, E.; Bläs, R.; Lauer, S.; Winkler, H. *J. Chem. Phys.* **1985**, *82*, 3584.
(40) Winkler, H.; Bill, E.; Lauer, S.; Lauer, U.; Trautwein, A. X.; Kostikas, A.; Papaefthmyiou, V.; Bögge, H.; Müller, A.; Gerdau, E.; Gonser, U. *J. Chem. Phys.* **1985**, *82*, 3594.
(41) Boyd, P. D. W., unpublished calculations.

density at the tungsten atoms is small. However the α spin is substantially localized on the iron atom in each case.

The overall charge distributions for molecules $[Fe(MoS_4)_2]^{3-}$ and $[Fe(WS_4)_2]^{2-/3-}$ are quite similar. This paradox is seen in Table IVa to arise from the subtle but significant redistribution of electron density between the d^6 and d^7 molecules. Further, the calculated charge distribution for the hypothetical one-electron-oxidized species $[Fe(MoS_4)_2]^{2-}$ is also similar to that of the anion.[41] A detailed comparison between $[Fe(MoS_4)_2]^{2-}$ and $[Fe(MoS_4)_2]^{3-}$ indicates that the extra electron is distributed over the whole complex (Fe (0.143), Mo (0.07), S_B (0.065), S_T (0.113)) with about 85% of the added charge residing on the tetrathiomolybdate ligands.[42] A similar effect is also found for the $[Fe(WS_4)_2]^{2-/3-}$ anions (Table IV). This leads to a ready interpretation of the Mössbauer spectra of these complexes. The observed isomer shifts in the $[Fe(WS_4)_2]^{2-/3-}$ anions[39,39] of 0.44 and 0.45 mm/s indicate little change in charge on the iron nucleus[43] while the quadrupole splittings, 2.65 and 1.03 mm/s, indicate significant changes in the iron orbital populations.[40] In the case of the $[Fe(WS_4)_2]^{2-/3-}$ couple studied here there are indeed significant changes in the iron d orbital populations even though they lead to a similar overall charge on the iron atom (see Table IVa).

A puzzling feature of the bis(tetrathiomolybdate) and bis(tetrathiotungstate) complexes is that while both the dianionic and trianionic species may be isolated for tungsten,[23,44] only the trianion has been isolated for molybdenum. Electrochemical studies have shown the oxidation of $[Fe(MoS_4)_2]^{3-}$ to be irreversible in acetonitrile, and the stability of the $[Fe(WS_4)_2]^{2-}$ ion compared with the $[Fe(MoS_4)_2]^{2-}$ ion has been ascribed to greater thermal stability and stronger binding of the tetrathiotungstate ion.[5,6] The spin-polarized energy level scheme for $[Fe(MoS_4)_2]^{3-}$ suggests that oxidation should occur at the HOMO, the $7b_2^{\beta}$ orbital in Figure 6, leaving the complex in a quintet ($S = 2$) state similar to that found for $[Fe(WS_4)_2]^{2-}$. This leads to a similar d^6 configuration as is found in the iron(II) complex $[Fe(MoS_4)(SH)_2]^{2-}$.[19] The stable configuration for $[Fe(MoS_4)_2]^{2-}$ (tested by transition-state calculations) is the latter. The analogous $[Fe(WS_4)_2]^{2-}$ has four unpaired electrons[23] as would be expected for oxidation of an electron from the xy orbital.

(42) Calculation on $[Fe(MoS_4)_2]^{2-}$ with same geometry as for $[Fe(MoS_4)_2]^{3-}$ and Watson sphere of charge 2+. Charge distribution: Fe (s, 0.537; p, 0.682; d, 7.029), Mo (s, 0.468; p, 0.536; d, 4.409), S_B (s, 1.841; p, 4.409), S_T (s, 1.842; p, 4.641).

(43) This is supported by very similar calculated charge densities at the iron nucleus (spin polarized) of 11 876.297 and 11 875.974 au, respectively.

(44) Coucouvanis, D.; Baenziger, N. C.; Stremple, P. *J. Am. Chem. Soc.* **1981**, *103*, 4601.

Conclusions

Magnetization studies show unequivocally that $[Fe(MoS_4)_2]^{3-}$ has an $S = {}^3/_2$ ground state with a significant positive zero-field splitting. This is in accord with conclusions based on esr spectroscopy.

Scattered wave-SCF-Xα calculations are turning out to be useful indicators of the nature of the valence orbitals in thiomolybdate complexes. They reveal that formal oxidation states and d^n configurations retain a useful degree of meaning despite contradictory isomer shift data. For $[Fe(MoS_4)_2]^{3-}$, an iron(I) formulation is favored rather than the iron(III) formulation suggested by Mössbauer spectroscopy.

Acknowledgment. Work at the University of Southern California was supported by NSF Grants CHE 8026812 and CHE 8519913 and at Battelle Kettering by USDA Grant 81-CRCR-1-0675. P.D.W.B. thanks the University of Auckland for Research and Study Leave during which this project was initiated.

Supplementary Material Available: Tables II and III containing magnetic susceptibility data and orbital energies and populations (6 pages). Ordering information is given on any current masthead page.

Contribution from the Chemistry Department, University of Florida, Gainesville, Florida 32611

E and *C* Parameters from Hammett Substituent Constants and Use of *E* and *C* To Understand Cobalt–Carbon Bond Energies

Russell S. Drago,* Ngai Wong, Carl Bilgrien, and Glenn C. Vogel[1]

Received September 8, 1986

An updated list of *E* and *C* parameters was calculated from a larger data base than that used in an earlier fit. The new data base included 42 acids, 55 bases, and about 500 data points. We also report best-fit parameters for 13 enthalpy–frequency shift relations. From this updated list, we have discovered relationships which lead to equations that enable one to calculate *E* and *C* parameters from Hammett substituent constants for a series of substituted phenols and pyridines. This procedure provides a simple method for greatly increasing the number of acids and bases included in the correlation. An *E* and *C* analysis was used to study the dissociation energy of the cobalt–carbon bond in alkyl-substituted bis(dimethylglyoximato)cobalt(II) complexes. This analysis gave calculated dissociation energies that were within experimental error of the measured values and gave a value for cobalt–carbon bond dissociation for the unligated complex. The basic procedure allows for the incorporation of ligand influence on bond dissociation energies into the correlation.

Introduction

The correlation of enthalpies of adduct formation, ΔH, by eq 1 has proven to be a powerful tool in understanding and predicting the interaction between Lewis acids (acceptors) and bases (donors).[2] In eq 1, the *E* and *C* parameters are related to electrostatic

$$-\Delta H + W = E_A E_B + C_A C_B \quad (1)$$

and covalent interactions, respectively, A and B are subscripts referring to an acceptor and a donor, respectively, and W is any constant enthalpy contribution to ΔH associated with a given acceptor reacting with a series of donors or a given donor reacting with a series of acceptors. In most systems studied to date, $W = 0$.

One current objective in this area of chemistry involves expanding the applicability[3,4] and number of donors and acceptors included in this model. One of the barriers to expanding the

(1) On sabbatical leave from Ithaca College, Ithaca, NY.

(2) Drago, R. S. *Coord. Chem. Rev.* **1980**, *33*, 251 and references therein.

(3) Drago, R. S.; Kroeger, M. K.; Stahlbush, J. R. *Inorg. Chem.* **1981**, *20*, 306.

(4) Doan, P. E.; Drago, R. S. *J. Am. Chem. Soc.* **1984**, *106*, 2772.

0020-1669/87/1326-0009$01.50/0